

LETTER TO THE EDITOR

Total cross sections for electrons and positrons colliding with H₂O molecules

O Sueoka, S Mori and Y Katayama

Institute of Physics, College of Arts and Sciences, University of Tokyo, 3-8-1 Komaba, Meguro-ku, Tokyo 153, Japan

Received 28 February 1986

Abstract. The total cross sections for 1-400 eV electrons and positrons colliding with H₂O molecules have been measured using a TOF method. The results for electron collisions were compared with positron collision data and with previous electron collision work. Data for electron scattering and positron scattering almost coincide with each other in the energy ranges above 200 eV and below 2 eV.

Although electron collisions with H₂O molecules are very important in various phenomena, measurements of total cross sections for electrons are few. Measurements for positron collisions have not yet been performed. In order to investigate the collision process in H₂O molecules and to offer data for the absorption coefficient, total cross sections for electron and positron collisions with H₂O have been measured using the same experimental procedure and apparatus. The H₂O molecule is well known as a typical polar molecule (of polarisability 1.85 D). The differential cross section measurements of Jung *et al* (1982) have shown that the scattering of electrons via rotational excitations shows a very sharp forward peaking.

A straight-type TOF apparatus with a flight path of 692 mm was used to measure the total cross sections. Details of the experimental set-up, experimental procedure and the method of data analysis were described in our previous papers (Sueoka and Mori 1984, 1986). The gas pressure in the collision cell was measured by a Baratron gauge, and was accurately controlled by a microcomputer. A vacuum run and a gas run were automatically alternated every 500 s. During the change-over from a gas run to a vacuum run, the measurement paused for 220 s because of the difficulty in evacuating the water vapour. For many gases other than water vapour, the pause is only 120 s for the present system. The values of the total cross sections were determined by a normalisation procedure to the e⁺-N₂ data of Hoffman *et al* (1982). A retarding potential method was applied to the TOF spectroscopy, in which the potential E_0 was zero for electron collisions and 1.5 eV for positron collisions, where E_0 is the difference of the retarding potential from the acceleration potential. The true signal spectrum was computed from raw TOF data by the method of Coleman *et al* (1974). The total cross section Q_t is given as follows:

$$Q_t = (\rho l)^{-1} \ln(I_v/I_g)$$

where I_v and I_g are the intensity in a vacuum run and that in a gas run, respectively, ρ is the density of the collision gas and l is the effective length of the collision cell.

The magnetic field, by which the projectile particles were transported, was mainly 4.5 G for electron beams in the vicinity of the collision cell, while in the range under 11 eV a magnetic field of 3 G was used. Data for the two versions in the range between 2 and 11 eV coincide well with each other. For positron beams, a magnetic field of 9 G was used, and in the range below 7 eV, measurements using a field of 4.5 G were also performed. Because of the weak intensity of our positron beams, the weaker magnetic field was not used. However, the condition may be sufficient for positron collisions, as described in a previous paper (Sueoka and Mori 1986). To check the influence of the magnetic field used for electron collisions, the magnetic-field dependence of the total cross sections was investigated in the low-energy range. The results

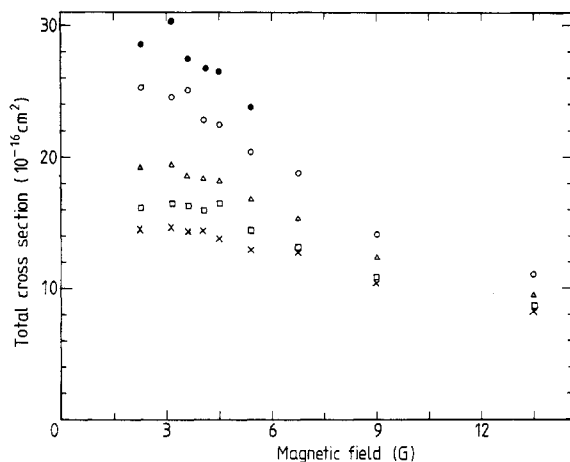


Figure 1. Total cross section values plotted against the magnetic field for the beam transportation in electron collisions. ●, 1.0 eV; ○, 1.2 eV; △, 1.6 eV; □, 2.0 eV; ×, 2.5 eV.

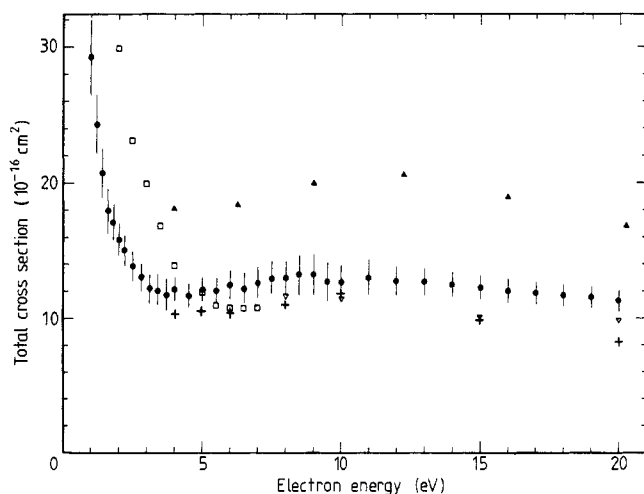


Figure 2. Total cross sections for electrons colliding with H_2O molecules at low energies: ●, the present experimental results; ▲, Brüche (1929); □, Sokolov and Sokolova (1981); +, the integrated elastic cross section of Danjo and Nishimura (1985); ▽, the calculated data of Hayashi (1983). The error bars show the uncertainties in the present results excluding the systematic error.

for the total cross sections plotted against the magnetic field for several impact energies are shown in figure 1. In conclusion, the present total cross section data for 3 and 4.5 G in the related energy ranges of electron collisions were only slightly affected by the magnetic field.

The total cross sections for electrons colliding with H_2O in the range below 20 eV have been obtained. The present data are shown in figure 2 together with the experimental results of Brüche (1929), Sokolov and Sokolova (1981), the data of Hayashi

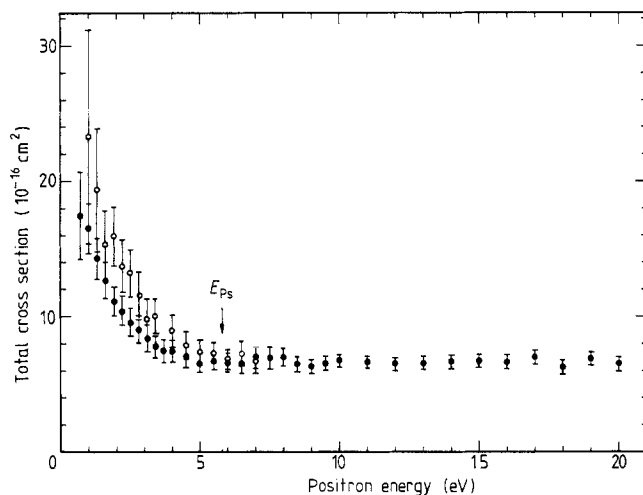


Figure 3. Total cross sections for positrons colliding with H_2O molecules. The upper data for the 4.5 G magnetic field (\circ) should be adopted in the low energy range. The data for 9 G (\bullet) in this range are merely shown as a reference.

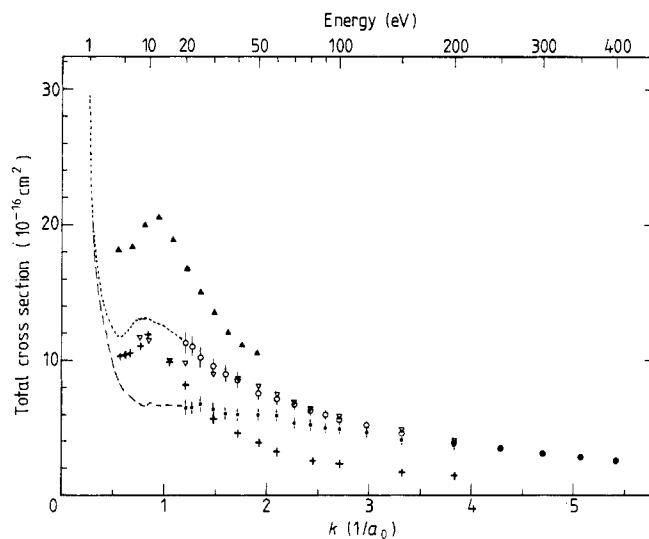


Figure 4. Total cross sections for electrons and positrons extending to intermediate energies. The present results: \bullet , positrons; \circ , electrons; \blacktriangle , the experimental data of Brüche (1929); $+$, the integrated elastic cross section of Danjo and Nishimura (1985); ∇ , the data of Hayashi (1983) determined from electron beam and electron swarm data. The dotted and broken curves represent the visually fitted curve of the present data given in figures 2 and 3.

(1983) determined from electron beam and electron swarm data, and the integrated elastic cross sections of Danjo and Nishimura (1985). As expected at low energies, the values of the total cross sections increase with decreasing impact energy. In the range below 1 eV, the results of Sokolov and Sokolova (1981) presented very high-value data points. A shallow minimum $Q_{\min}^- = (12.0 \pm 0.9) \times 10^{-16} \text{ cm}^2$ in the total cross section curve is shown at 4.5 eV. A broad and inconspicuous peak around 10 eV, $Q_{\max}^- = (13.2 \pm 1.1) \times 10^{-16} \text{ cm}^2$, follows the minimum. Part of the total cross section at these energy ranges is due to the scattering by the negative-ion state in H_2O which has a broad peak at 6–8 eV (Seng and Linder 1976).

The results for positron collisions in the range below 20 eV are presented in figure 3. The data below 7 eV were obtained using a field of 4.5 G, and those above 7.5 eV using a field of 9 G. In the range below 7 eV, data for 9 G are displayed as a reference. The results in the range below 2 eV almost coincide with the results of the electron collisions. In the range below 5 eV, the smooth decreasing curve with increasing impact energy is shown. Even in the range above the threshold of positronium formation ($E_{\text{Ps}} = 5.8 \text{ eV}$) the increase in the total cross sections observed in many other gases is not present. The minimum in the total cross section curve for positron collisions is also not present. This may be due to the low probability of positronium formation in a strong dipole field with increasing localisation of the negative electric charge

Table 1. Total cross sections for electron collisions (10^{-16} cm^2). The cross section values in the energy range 1.0–11.0 eV are taken from the 3 G measurement, and the others are taken from the 4.5 G measurement.

Energy (eV)	Cross section	Energy (eV)	Cross section
1.0	29.2 ± 2.8	13.0	12.7 ± 1.0
1.2	24.3 ± 2.2	14.0	12.5 ± 0.9
1.4	20.7 ± 1.8	15.0	12.3 ± 0.9
1.6	17.9 ± 1.6	16.0	12.0 ± 0.9
1.8	17.1 ± 1.3	17.0	11.8 ± 0.9
2.0	15.8 ± 1.2	18.0	11.7 ± 0.8
2.2	15.0 ± 1.1	19.0	11.6 ± 0.8
2.5	13.9 ± 1.1	20.0	11.3 ± 0.8
2.8	13.0 ± 1.0	22.0	11.0 ± 0.8
3.1	12.2 ± 1.0	25.0	10.2 ± 0.8
3.4	12.0 ± 1.0	30.0	9.5 ± 0.7
3.7	11.7 ± 1.1	35.0	9.0 ± 0.6
4.0	12.2 ± 0.9	40.0	8.5 ± 0.6
4.5	11.7 ± 0.8	50.0	7.5 ± 0.5
5.0	11.9 ± 0.9	60.0	7.1 ± 0.4
5.5	12.0 ± 1.0	70.0	6.7 ± 0.4
6.0	12.5 ± 1.1	80.0	6.3 ± 0.4
6.5	12.3 ± 1.1	90.0	6.0 ± 0.3
7.0	12.6 ± 1.1	100	5.6 ± 0.3
7.5	13.0 ± 1.2	120	5.2 ± 0.3
8.0	13.0 ± 1.2	150	4.6 ± 0.2
8.5	13.3 ± 1.4	200	4.0 ± 0.2
9.0	13.2 ± 1.5	250	3.5 ± 0.2
9.5	12.7 ± 1.4	300	3.2 ± 0.2
10.0	12.7 ± 1.3	350	2.9 ± 0.2
11.0	13.0 ± 1.4	400	2.6 ± 0.1
12.0	12.8 ± 1.1		

(Goldanskii 1968). Another reason for the absence of a minimum is merely the large size of the cross sections in the low-energy range. The increase of the total cross section due to ionisation is not seen explicitly.

The total cross sections for electrons and positrons in the range between 20 and 400 eV are plotted against the wavenumber k in figure 4 together with the experimental data of Brüche (1929), the integrated elastic cross section of Danjo and Nishimura (1985) and the data of Hayashi (1983) determined from electron beam and electron swarm data. In the range above 200 eV the data for positron collisions merge into the electron collision data, for example those measured in the hydrocarbon molecules by Sueoka and Mori (1986). Brüche's data are somewhat higher than others. The present electron collision data almost coincide with those of Hayashi (1983), which were obtained by calculation from electron beam and electron swarm data for the range between 8 and 200 eV.

As shown in figures 2, 3 and 4, the tendency of the total cross sections for electrons and positrons to merge was also observed below 2 eV. This may be related to the fact that H_2O is a polar molecule. Actually, for this molecule, rotational excitations by electron impact are considered to be the dominant scattering mechanism at low energies (Jung *et al* 1982), and it has been shown that rotational excitations by electron impact can be well described by first-order Born scattering theory (Jain and Thompson 1983). We look forward to the theoretical calculation of the total cross sections for both electrons and positrons.

Table 2. Total cross sections for positron collisions (10^{-16} cm^2). The cross section values in the energy range 1.0–7.0 eV are taken from the 4.5 G measurement, and the others are taken from the 9 G measurement.

Energy (eV)	Cross section	Energy (eV)	Cross section
1.0	23.3 ± 7.9	14.0	6.6 ± 0.5
1.3	19.3 ± 4.6	15.0	6.7 ± 0.5
1.6	15.3 ± 2.5	16.0	6.6 ± 0.5
1.9	15.9 ± 2.2	17.0	7.0 ± 0.5
2.2	13.7 ± 2.0	18.0	6.2 ± 0.5
2.5	13.2 ± 1.8	19.0	6.9 ± 0.5
2.8	11.6 ± 1.8	20.0	6.5 ± 0.5
3.1	9.8 ± 1.5	22.0	6.5 ± 0.5
3.4	10.0 ± 1.4	25.0	6.7 ± 0.5
4.0	8.9 ± 1.2	30.0	6.4 ± 0.4
4.5	7.9 ± 1.0	35.0	6.1 ± 0.4
5.0	7.4 ± 0.9	40.0	6.0 ± 0.4
5.5	7.3 ± 0.9	50.0	6.0 ± 0.5
6.0	6.9 ± 0.7	60.0	5.9 ± 0.4
6.5	7.3 ± 0.9	70.0	5.4 ± 0.4
7.0	6.8 ± 1.0	80.0	5.3 ± 0.4
7.5	6.9 ± 0.8	90.0	5.0 ± 0.4
8.0	7.0 ± 0.7	100	4.9 ± 0.4
8.5	6.5 ± 0.6	120	4.6 ± 0.3
9.0	6.3 ± 0.5	150	4.0 ± 0.3
9.5	6.6 ± 0.5	200	3.6 ± 0.3
10.0	6.7 ± 0.5	250	3.5 ± 0.3
11.0	6.6 ± 0.4	300	3.2 ± 0.2
12.0	6.5 ± 0.5	350	2.8 ± 0.2
13.0	6.6 ± 0.5	400	2.6 ± 0.2

Values of the total cross section are given in tables 1 and 2. The error shown was obtained by the addition of $\Delta I/I$, $\Delta\rho/\rho$ and $\Delta l/l$, not including the systematic error, where I means $\ln(I_v/I_g)$, and ΔI includes all the statistical errors in the counting.

The authors would like to thank Professor M Hayashi for sending his data before publication.

References

- Brüche E 1929 *Ann. Phys., Lpz* **1** 93–134
Coleman P G, Griffith T C and Heyland G R 1974 *Appl. Phys.* **5** 223–30
Danjo A and Nishimura H 1985 *J. Phys. Soc. Japan* **54** 1224–7
Goldanskii V I 1968 *At. Energy Rev.* **6** 3–148
Hayashi M 1983 private communication
Hoffman K R, Dababneh M S, Hsieh Y-F, Kauppila W E, Pol V, Smart J H and Stein T S 1982 *Phys. Rev. A* **25** 1393–403
Jain A and Thompson D G 1983 *J. Phys. B: At. Mol. Phys.* **16** 3077–98
Jung K, Antoni Th, Muller R, Kochem K-H and Ehrhardt H 1982 *J. Phys. B: At. Mol. Phys.* **15** 3535–55
Seng G and Linder F 1976 *J. Phys. B: At. Mol. Phys.* **9** 2539–51
Sokolov V F and Sokolova Yu A 1981 *Sov. Tech. Phys. Lett.* **7** 268–9
Sueoka O and Mori S 1984 *J. Phys. Soc. Japan* **53** 2491–500
—— 1986 *J. Phys. B: At. Mol. Phys.* to be published